



King's Research Portal

DOI:

[10.1016/j.mee.2017.01.005](https://doi.org/10.1016/j.mee.2017.01.005)

Document Version

Publisher's PDF, also known as Version of record

[Link to publication record in King's Research Portal](#)

Citation for published version (APA):

Kohl, D., Mesquida, P., & Schitter, G. (2017). Quantitative AC - Kelvin Probe Force Microscopy. *MICROELECTRONIC ENGINEERING*, 176, 28-32. <https://doi.org/10.1016/j.mee.2017.01.005>

Citing this paper

Please note that where the full-text provided on King's Research Portal is the Author Accepted Manuscript or Post-Print version this may differ from the final Published version. If citing, it is advised that you check and use the publisher's definitive version for pagination, volume/issue, and date of publication details. And where the final published version is provided on the Research Portal, if citing you are again advised to check the publisher's website for any subsequent corrections.

General rights

Copyright and moral rights for the publications made accessible in the Research Portal are retained by the authors and/or other copyright owners and it is a condition of accessing publications that users recognize and abide by the legal requirements associated with these rights.

- Users may download and print one copy of any publication from the Research Portal for the purpose of private study or research.
- You may not further distribute the material or use it for any profit-making activity or commercial gain
- You may freely distribute the URL identifying the publication in the Research Portal

Take down policy

If you believe that this document breaches copyright please contact librarypure@kcl.ac.uk providing details, and we will remove access to the work immediately and investigate your claim.



Research paper

Quantitative AC - Kelvin Probe Force Microscopy

Dominik Kohl^{a,*}, Patrick Mesquida^{a,b}, Georg Schitter^a^aAutomation and Control Institute (ACIN), Technical University of Vienna, Gusshausstr. 27-29/E376, Vienna 1040, Austria^bDepartment of Physics, King's College London, London, United Kingdom

ARTICLE INFO

Article history:

Received 13 October 2016

Received in revised form 27 December 2016

Accepted 10 January 2017

Available online 12 January 2017

Keywords:

SPM

AFM

KPFM

DC free

Surface potential

ABSTRACT

This paper presents a novel feedback based Scanning Probe Microscopy method which enables quantitative surface potential measurements without the need of the DC bias of Kelvin Probe Force Microscopy. In addition to the sinusoidal excitation signal at frequency ω , a sinusoidal signal with the frequency 2ω is applied to the conductive cantilever. By modulating the amplitude of the signal at 2ω , the resulting electric force component at the frequency ω can be nullified by a feedback controller. When the force and, hence, the cantilever oscillation is zero, the required amplitude represents the quantitative surface potential. Recording this amplitude while scanning over the sample allows to acquire a two dimensional map of the surface potential. The AC-KPFM method, shown analytically and with experimental results, keeps the compensation based principle of classical KPFM, resulting in quantitative measurements but without the need of a DC bias.

© 2017 The Authors. Published by Elsevier B.V. This is an open access article under the CC BY license (<http://creativecommons.org/licenses/by/4.0/>).

1. Introduction

Atomic force microscopes (AFM) [1] are important tools for topography and surface characterization on the molecular and atomic level. Various research fields such as biology, physics or materials science [2] are using functional imaging-modes like Kelvin Probe Force Microscopy (KPFM) [3,4]. With KPFM as presented first in [5], it is possible to map the sample surface potential in a quantitative way with nanometer resolution. In the following this method is referred to as classical KPFM.

Most KPFM methods are two stage processes. In a first run a sharp conductive tip mounted on a micro-mechanical cantilever scans over the sample in order to track and record its topography in intermittent-contact mode. An optical deflection readout system [6] detects the mechanically excited amplitude of the cantilever oscillation. A feedback controller keeps the deflection amplitude constant by moving the sample in opposite direction [7]. The required compensation motion equals the sample topography and is stored for the second run.

By following this topography in a few nanometer distance h in a second run [5] the quantitative surface potential $\Phi = \Phi(x, y)$ can be recorded. As shown in Fig. 1 a sinusoidal electrical signal with amplitude a and frequency ω is applied to a conductive cantilever at its

mechanical resonance frequency. Together with an adjustable DC-potential U_{DC} , the voltage between tip and sample can be written as:

$$U(t) = \Phi - U_{DC} + a \sin(\omega t). \quad (1)$$

The resulting electric force acting on the cantilever is then:

$$F(t) = \frac{1}{2} \frac{\partial C}{\partial h} U(t)^2 \quad (2)$$

where $\frac{\partial C}{\partial h}$ is the capacitance gradient of the entire cantilever-sample system. Inserting Eq. (1) into Eq. (2) leads to:

$$F(t) = \frac{1}{2} \frac{\partial C}{\partial h} \left\{ (\Phi - U_{DC})^2 + \frac{a^2}{2} + 2a(\Phi - U_{DC}) \sin(\omega t) - \frac{a^2}{2} \cos(2\omega t) \right\} \quad (3)$$

It can be seen that the force component at the frequency F_ω vanishes when $\Phi - U_{DC} = 0$, i.e., no cantilever oscillation occurs when the DC-potential U_{DC} equals the surface potential Φ [8]. In classical KPFM a feedback controller continuously adjusts U_{DC} such that the ω -component of the force F_ω (second term in curly brackets), hence the cantilever oscillation is zero thereby providing $\Phi = U_{DC}$. With this compensation based measurement method a quantitative

* Corresponding author.

E-mail address: kohl@acin.tuwien.ac.at (D. Kohl).

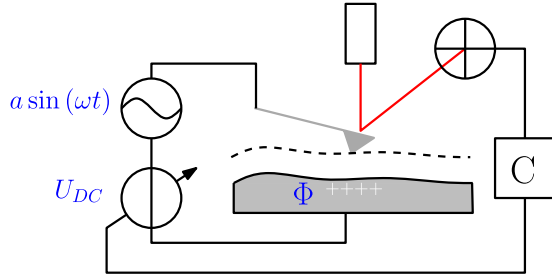


Fig. 1. A sinusoidal excitation signal $a \sin(\omega t)$ is applied to the conductive AFM cantilever. The DC voltage U_{DC} is adjusted via the feedback controller C and compensates the positive surface potential Φ indicated with + + + +.

surface potential map can be created by recording $U_{DC}(x, y)$ as a function of the lateral position (x, y) . However, certain semiconductors [9], sensors [10] or catalysts show a DC voltage dependence, and biomolecules often have to be studied in water (in vitro) [3], where a DC voltage would lead to unwanted electrochemical reactions [11,12]. The required DC bias complicates, influences, or even makes quantitative surface potential measurements impossible on such samples.

A possibility to overcome this limitation is to utilize “open-loop” or “Dual Harmonic” KPFM methods, which do not require DC-bias feedback [13–16]. These methods apply a single sinusoidal excitation potential $\sin(\omega t)$ to the cantilever and observe the resultant amplitude of vibration at the frequency ω and 2ω . The surface potential is computed by comparing these two amplitudes. The advantage is that no DC-bias and no feedback controller is required. However, they require correction factors for the used excitation amplitude as well as cantilever dynamic and readout sensitivity at the frequencies ω and 2ω . These factors need to be determined with control experiments for calibration. Next to inevitable uncertainties and potential non-linearities, these factors can also change due to drift or changing environmental conditions during the measurement and could lead to measurement errors.

Alternatively methods like “G-Mode KPFM” or “Band excitation KPFM” [17–19] analyze the spectral response of the cantilever vibration. Similar to the methods presented before, they compute the surface potential by comparing the ω and 2ω response of the cantilever, acquired by a fast Fourier transform. The advantage is that no Lock-In amplifiers and feedback controller are required. However, next to a computationally intensive fast Fourier transform and a huge amount of data, these methods also require the same correction factors for excitation amplitude, cantilever dynamic and readout sensitivity.

The AC-KPFM method proposed in this paper shows a novel approach, which enables feedback based quantitative surface potential measurements without the need of a DC-bias and calibration. After deriving the basic principle and the physical model in Section 2, analytical investigations of the control sensitivity are performed. A custom made experimental setup which extends commercial AFM systems from classical KPFM to AC-KPFM is presented in Section 3, showing experimental results in Section 4, followed by a conclusion.

2. Proposed approach: AC-KPFM

In order to avoid the unwanted DC-component (U_{DC}) of classical KPFM, an additional sinusoidal voltage with amplitude b and frequency 2ω is applied instead of U_{DC} :

$$U(t) = \Phi + a \sin(\omega t) - b \cos(2\omega t). \quad (4)$$

Inserting Eq. (4) into Eq. (2) yields the following force acting on the AFM cantilever:

$$F = \frac{1}{2} \frac{\partial C}{\partial h} \left\{ \begin{aligned} &\Phi^2 + \frac{a^2 + b^2}{2} \\ &+ [2\Phi a + ab] \sin(\omega t) \\ &- [2\Phi b - \frac{a^2}{2}] \cos(2\omega t) \\ &- ab \sin(3\omega t) \\ &+ \frac{b^2}{2} \cos(4\omega t) \end{aligned} \right\} \quad (5)$$

Similar to classical KPFM, the force component at the frequency ω (second term in the curly brackets) can be controlled to zero. By regulating the amplitude b with a feedback controller it can be ensured that $2\Phi a + ab = 0$. The surface potential to be determined can then be calculated as $\Phi = -\frac{b}{2}$. In the following this method is called AC-KPFM $_{\omega}$.

As can be seen from Eq. (5), the force component at the frequency 2ω can also be regulated to zero (third term in the curly brackets). The two methods to achieve this are referred to in the following as AC-KPFM $_{2\omega,a}$ and AC-KPFM $_{2\omega,b}$, indicating that $F_{2\omega}$ is nullified by adjusting either the amplitude a or the amplitude b respectively. In both variations the surface potential is calculated with $\Phi = \frac{a^2}{4b}$. As can be seen for AC-KPFM $_{2\omega,b}$ a singularity occurs for a surface potential of zero, which makes this method unsuitable for feedback operation.

In a next step the KPFM and control sensitivity of the three AC-KPFM methods are compared with classical KPFM. First, the KPFM sensitivity $S_{KPFM} = \frac{\partial F}{\partial \Phi}$ is analyzed. This is performed with the feedback controller switched off. Inserting Eq. (3) for classical KPFM and Eq. (5) for the AC-KPFM variations:

$$\begin{aligned} S_{KPFM} &= \frac{\partial F_{\omega}}{\partial \Phi} = \frac{\partial C}{\partial h} a \\ S_{AC-KPFM_{\omega}} &= \frac{\partial F_{\omega}}{\partial \Phi} = \frac{\partial C}{\partial h} a \\ S_{AC-KPFM_{2\omega,a}} &= \frac{\partial F_{2\omega}}{\partial \Phi} = \frac{\partial C}{\partial h} b \\ S_{AC-KPFM_{2\omega,b}} &= \frac{\partial F_{2\omega}}{\partial \Phi} = 0 \end{aligned} \quad (6)$$

As can be seen from Eq. (6) the KPFM sensitivity is equal for the first three methods and depends on the capacitance gradient $\frac{\partial C}{\partial h}$ and amplitude (a or b) of the applied sinusoidal excitation signal. Except AC-KPFM $_{2\omega,b}$ where the sensitivity is zero, caused by the previously explained singularity.

However, there is a difference in control sensitivity which is defined by the control signal (controller output) required to compensate for the surface potential. For classical KPFM the DC-potential is used for compensation ($S_{cont} = \frac{U_{DC}}{\Phi}$). For the three proposed versions AC-KPFM $_{\omega}$, AC-KPFM $_{2\omega,a}$ and AC-KPFM $_{2\omega,b}$ the control sensitivity is defined by $S_{cont} = \frac{b}{\Phi}$, $S_{cont} = \frac{a}{\Phi}$ and $S_{cont} = \frac{b}{\Phi}$ respectively. The comparison of the control sensitivities is plotted in Fig. 2.

Following Eq. (5) S_{cont} for AC-KPFM $_{\omega}$ is linear and twice as high as in classical KPFM. An even higher but non-linear control sensitivity is obtained for small surface potentials with AC-KPFM $_{2\omega,a}$ nullifying the $F_{2\omega}$ -component. The AC-KPFM $_{2\omega,b}$ also nullifying the $F_{2\omega}$ -component follows a hyperbolic curve with a singularity at $\Phi = 0$. Although AC-KPFM $_{2\omega,a}$ offers a higher sensitivity than AC-KPFM $_{\omega}$, its non-linearity is a significant drawback for feedback operation.

From this analytical investigation it can be concluded that the AC-KPFM $_{\omega}$ shows a twice as high linear control sensitivity which makes it best suited for closed-loop operation. In the following section the experimental results are shown.

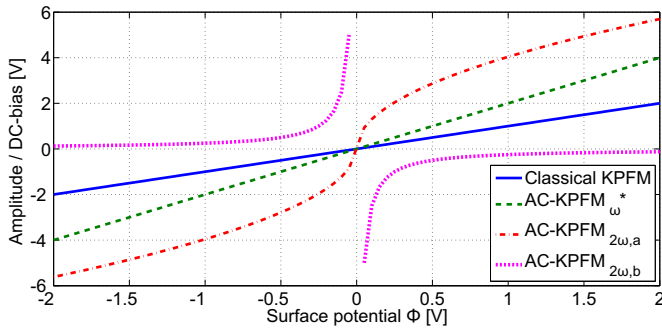


Fig. 2. AC-KPFM_ω (green curve) linear and twice as high control sensitivity in comparison with classical KPFM (blue solid line). *For better visibility the sensitivity of AC-KPFM_ω is inverted. AC-KPFM_{2ω,a} (red dash dotted curve) follows a square-root dependence. AC-KPFM_{2ω,b} (magenta small dotted curve) offers an hyperbolic behavior with a singularity at $\Phi = 0$. A negative amplitude equals a phase shift of 180° for the corresponding sinusoidal signal.

3. Experimental setup

To demonstrate the proposed AC-KPFM versions an experimental setup is built based on a commercial AFM (Multimode 8, Bruker, Santa Barbara, USA) equipped with a signal access module (SAM). In order to show the working principles of the previously presented AC-KPFM versions, the control sensitivity is measured individually. For this test a dual channel function generator (Agilent 33500B, Santa Rosa, USA) is connected via the SAM to a conductive AFM cantilever (RFESP, $f_0 = 90$ kHz, $k = 3$ N/m, Bruker, Santa Barbara, USA) providing the two required sinusoidal signals. A DC voltage source is connected via the same SAM to a conductive flat silica sample to simulate a well known surface potential. By adjusting the amplitudes (a or b) of the three proposed AC-KPFM versions until the corresponding force (F_ω or $F_{2\omega}$) is nullified, the control sensitivity is acquired. Fig. 3 shows the experimental results compared with simulation. It is clearly visible that the experimental measurements are in good accordance to simulation.

To be able to record full AC-KPFM surface potential maps with the existing commercial AFM system, a custom made printed circuit board (PCB) with off-the-shelf, analog electronic components is built. Because of its linearity and simpler integration, AC-KPFM_ω version is chosen to realize Eq. (5) for demonstration. The custom made PCB containing standard operational amplifiers and analog multiplier ICs is connected via the SAM to the Multimode AFM controller. Fig. 4 shows a block diagram of the electronic board that extends the commercial AFM to an AC-KPFM imaging system. The two stage process of KPFM including topography recording and following of this topography is done with the built in functions of the AFM controller. Also

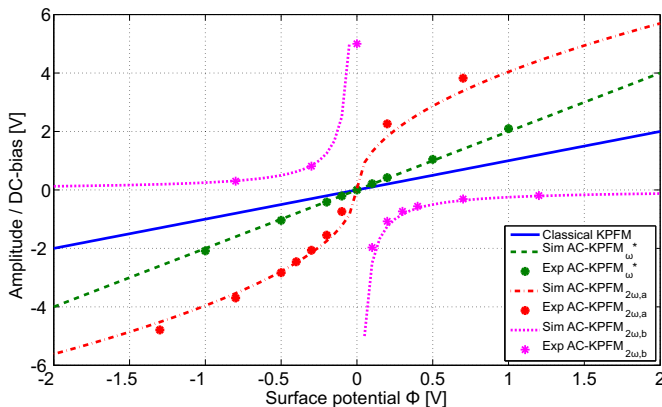


Fig. 3. Experimental results of the control sensitivity for the AC-KPFM variations are in good accordance to the derived theory.

feedback operation with the controller output $U_{DC} = b$ and excitation signal ($a \sin(\omega t)$) are realized with the Multimode controller. The voltage signals from the controller are connected to the input of the custom made PCB. This signal is split via high and low pass filter into DC-bias ($U_{DC} = b$) and excitation signal ($a \sin(\omega t)$) (see Fig. 4). By analog multiplication of the excitation signal with itself, the double frequency signal ($\cos(2\omega t)$) is generated and fed to a second multiplier. This second multiplier modulates the amplitude of the 2ω signal with the previously separated controller output signal b .

After summing the two signals with an analog summing stage a capacitor removes the remaining DC-bias. Finally the generated AC-KPFM_ω signal is applied via the SAM to the AFM cantilever. With this setup the operator is now able to operate the Multimode AFM with the new AC-KPFM_ω method in the same way as classical KPFM, which is demonstrated in the next section.

4. Imaging results

As test sample a flat, featureless conductive surface is chosen, on which a pseudo-spatial potential contrast was created by applying a low-frequency rectangular voltage signal with an amplitude of $1 V_{pp}$ and a duty cycle of 20% to the surface.

Fig. 5 shows the amplitude b generated by the controller in response to the rectangular signal. As the rectangular signal is not synchronized with the scanning-motion of the AFM, it appears as oblique stripes in the surface potential image. It should be noted that b appears inverted and twice as high as the applied rectangular signal, which follows directly from the relation $\Phi = -\frac{b}{2}$. Although relatively strong signal amplitudes were used for this first test, the images clearly demonstrate that the temporal, surface potential variations can be picked up by the AC-KPFM method.

In order to demonstrate AC-KPFM_ω with a real sample, a rectangular charge pattern on a thin film of PMMA is produced. Such a pattern has no topography (other than the natural roughness of the PMMA) but shows a clear potential contrast. The geometry of the μm -sized pattern is large enough so that edge effects can be neglected. The procedure is similar to the one used in [20]. Briefly, a PMMA thin-film of approximately 100 nm to 200 nm thickness was spin-coated on a thin gold film thermally evaporated onto a piece of polished Si wafer. For charge-writing and subsequent imaging, the sample is placed directly on the electrically grounded sample stage of the Dimension AFM (Dimension Icon, Bruker, Santa Barbara, USA). For writing as well as imaging the same conductive tip is used (TAP150A, Bruker, Sb-doped Si, specific resistivity 0.01–0.025 $\Omega \text{ cm}$). Charge-writing is performed by scanning a rectangular area of $7 \times 3.5 \mu\text{m}$ in intermittent-contact mode with an oscillation amplitude of about 30 nm (128 scan lines, tip velocity 14 $\mu\text{m/s}$). Simultaneously rectangular voltage pulses of 10 V, 2.5 ms pulse length, and 50 Hz pulse frequency are applied to the cantilever. First, classical KPFM is performed with a lift height of 50 nm (Fig. 6 (A) and (B)). Subsequently, the same area is recorded with AC-KPFM_ω and identical scan settings (e.g. lift height, tip velocity, controller gains).

From the topography image (A) it can be seen that the charge-writing did not lead to any topographical modification of the surface. It can, therefore, be concluded that any KPFM images show the true surface potential and not a topography artifact. (B) shows the pattern recorded by classical KPFM. (C) and (D) show the subsequently recorded AC-KPFM_ω signals, where in (C) the AC-KPFM_ω amplitude (b) is shown. To compute the surface potential (Φ), this image needs to be multiplied by $-\frac{1}{2}$ (D), according to Eq. (5). As expected the comparison of (B) and (D) clearly demonstrates that AC-KPFM provides the same surface potential map as classical KPFM.

Summarizing it clearly has been shown that surface charges can be quantitatively measured without applying a DC-voltage to the cantilever by using the proposed AC-KPFM_ω method.

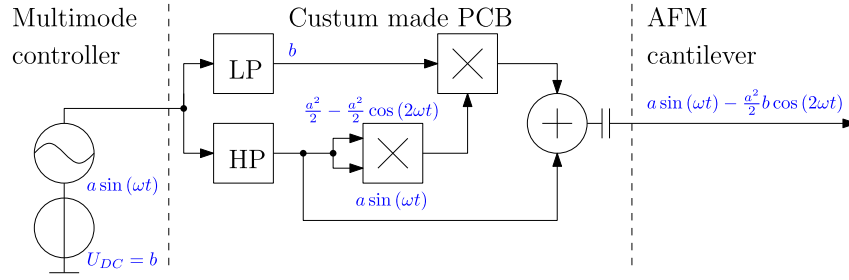


Fig. 4. Block diagram of the electronic board that extends a commercial AFM to AC-KPFM_ω nullifying the force component at F_{ω} by adjusting the amplitude b .

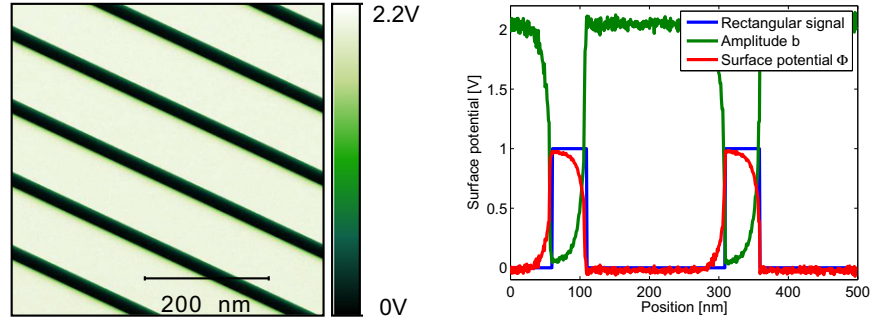


Fig. 5. Amplitude b of AC-KPFM_ω required to compensate a rectangular signal with an amplitude of 1 V_{pp} and a duty cycle of 20% indicated above the image. The quantitative surface potential Φ can be computed by inverting and scaling the signal by one half ($\Phi = -\frac{b}{2}$).

5. Conclusion

The presented compensation based AC-KPFM method enables quantitative surface potential measurements without the need of a

DC bias potential. It is investigated analytically and demonstrated with practical measurements that replacing the adjustable DC-potential by an amplitude modulated sinusoidal signal is feasible and offers an increased control sensitivity as compared to classical KPFM.

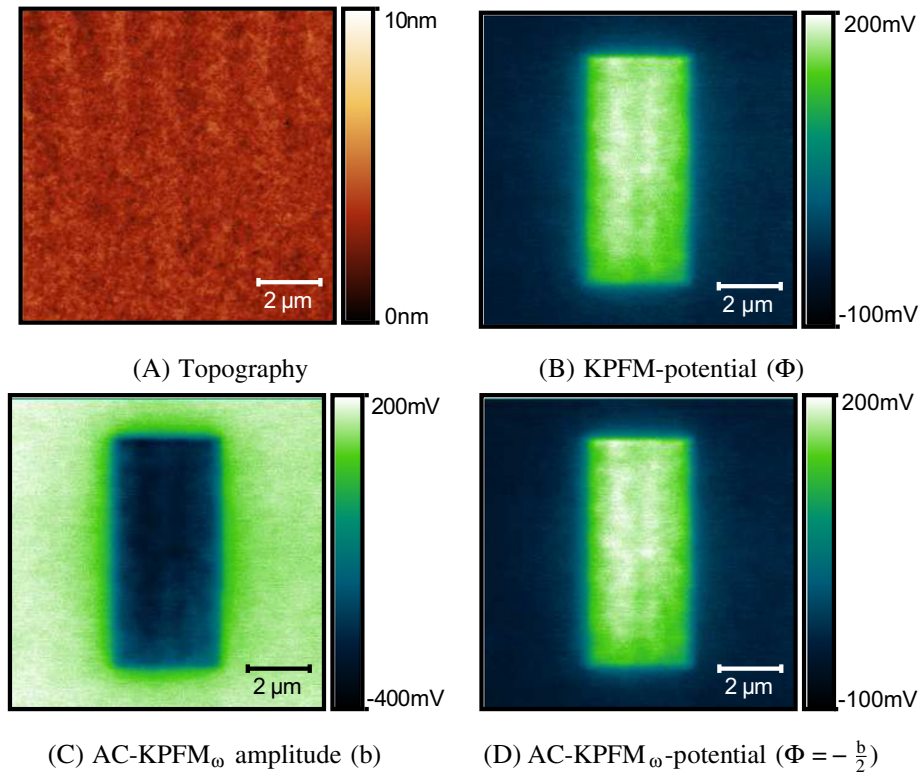


Fig. 6. Comparison of classical KPFM and AC-KPFM_ω of a positive charge pattern on PMMA. Topography (A) and surface potential Φ recorded with classical KPFM (B). (C) amplitude b and (D) surface potential $\Phi = -\frac{b}{2}$ acquired with AC-KPFM_ω of the same pattern as in (B). The images (C) and (D) were recorded immediately after (A) and (B) without disengaging the tip.

Measurements are performed on a flat sample with a pseudo-spatial potential contrast as well as of a positive pattern on PMMA showing comparable results to classical KPFM. This method opens the way to image the surface potential of various samples such as semiconductors or biological cells without the need for applying a disturbing or interfering DC-bias and enables new applications of feedback based KPFM technologies.

Acknowledgments

This work was funded by the Austrian Ministry for Transport, Innovation and Technology (FFG project number 837829). Open access for this article was funded by King's College London. We would like thank Simone Schuler from the Photonics Institute of TU Wien for providing the PMMA sample, and Christoph Kerschner for support with the electronics.

References

- [1] G. Binnig, C.F. Quate, C. Gerber, Atomic force microscope, *Phys. Rev. Lett.* 56 (9) (1986) 930–933.
- [2] N. Jalili, K. Laxminarayana, A review of atomic force microscopy imaging systems: application to molecular metrology and biological sciences, *Mechatronics* 14 (8) (2004) 907–945.
- [3] W. Melitz, J. Shen, A.C. Kummel, S. Lee, Kelvin probe force microscopy and its application, *Surf. Sci. Rep.* 66 (1) (2011) 1–27.
- [4] A.K. Sinensky, A.M. Belcher, Label-free and high-resolution protein/DNA nanoarray analysis using Kelvin probe force microscopy, *Nat. Nanotechnol.* 2 (10) (2007) 653–659.
- [5] M. Nonnenmacher, M. Boyle, H. Wickramasinghe, Kelvin probe force microscopy, *Appl. Phys. Lett.* 58 (25) (1991) 2921–2923.
- [6] G. Meyer, N.M. Amer, Novel optical approach to atomic force microscopy, *Appl. Phys. Lett.* 53 (24) (1988) 2400–2402.
- [7] R. Garcia, R. Perez, Dynamic atomic force microscopy methods, *Surf. Sci. Rep.* 47 (6) (2002) 197–301.
- [8] H. Jacobs, P. Leuchtmann, O. Homan, A. Stemmer, Resolution and contrast in Kelvin probe force microscopy, *J. Appl. Phys.* 84 (3) (1998) 1168–1173.
- [9] S.-Y. Chung, I.-D. Kim, S.-J.L. Kang, Strong nonlinear current-voltage behaviour in perovskite-derivative calcium copper titanate, *Nat. Mater.* 3 (11) (2004) 774–778.
- [10] B.D. Huey, D.A. Bonnell, Spatially localized dynamic properties of individual interfaces in semiconducting oxides, *Appl. Phys. Lett.* 76 (8) (2000) 1012–1014.
- [11] K.-i. Umeda, K. Kobayashi, N. Oyabu, Y. Hirata, K. Matsushige, H. Yamada, Practical aspects of Kelvin-probe force microscopy at solid/liquid interfaces in various liquid media, *J. Appl. Phys.* 116 (13) (2014) 134307.
- [12] L. Collins, S. Jesse, J.I. Kilpatrick, A. Tselev, O. Varennyk, M.B. Okatan, S.A. Weber, A. Kumar, N. Balke, S.V. Kalinin, Probing charge screening dynamics and electrochemical processes at the solid-liquid interface with electrochemical force microscopy, *Nat. Commun.* 5 (2014).
- [13] L. Collins, J. Kilpatrick, M. Bhaskaran, S. Sriram, S.A. Weber, S. Jarvis, B.J. Rodriguez, Dual harmonic Kelvin probe force microscopy for surface potential measurements of ferroelectrics, *Proceedings of ISAF-ECAPD-PFM 2012, IEEE, 2012*, pp. 1–4.
- [14] O. Takeuchi, Y. Ohrai, S. Yoshida, H. Shigekawa, Kelvin probe force microscopy without bias-voltage feedback, *Jpn. J. Appl. Phys.* 46 (8S) (2007) 5626.
- [15] N. Kobayashi, H. Asakawa, T. Fukuma, Nanoscale potential measurements in liquid by frequency modulation atomic force microscopy, *Rev. Sci. Instrum.* 81 (12) (2010) 123705.
- [16] N. Kobayashi, H. Asakawa, T. Fukuma, Quantitative potential measurements of nanoparticles with different surface charges in liquid by open-loop electric potential microscopy, *J. Appl. Phys.* 110 (4) (2011) 044315.
- [17] L. Collins, A. Belianinov, S. Somnath, N. Balke, S.V. Kalinin, S. Jesse, Full data acquisition in Kelvin Probe Force Microscopy: mapping dynamic electric phenomena in real space, *Sci. Rep.* 6 (2016).
- [18] L. Collins, J. Kilpatrick, S.A. Weber, A. Tselev, I.V. Vlassiouk, I.N. Ivanov, S. Jesse, S. Kalinin, B. Rodriguez, Open loop Kelvin probe force microscopy with single and multi-frequency excitation, *Nanotechnology* 24 (47) (2013) 475702.
- [19] L. Collins, A. Belianinov, S. Somnath, B.J. Rodriguez, N. Balke, S.V. Kalinin, S. Jesse, Multifrequency spectrum analysis using fully digital G Mode-Kelvin probe force microscopy, *Nanotechnology* 27 (10) (2016) 105706.
- [20] P. Mesquida, E.M. Blanco, R.A. McKendry, Patterning amyloid peptide fibrils by AFM charge writing, *Langmuir* 22 (22) (2006) 9089–9091.